Polarimetry Modeling

Ranjan Gupta

IUCAA, Post Bag 4, Ganeshkhind, Pune-411007

rag@iucaa.in

July 31 to August 8, 2017

Outline

- **Images of effects of dust and its composition**
- **Light Scattering Basics**
- **Scattering properties of composite grains and interstellar extinction – REAL DUST in Astrophysical Context**
- **Linear polarization calculations**
- **Abundance constraints**
- **IR emission from dust**
- **Laboratory Studies**

Role of Dust

Its is well known that the interstellar dust plays the most important role in which the light seen form stars suffers extinction. Conventional models assume Mie theory of light scattering with solid spheres and other shapes of silicate and graphite particles of different sizes. An extension of this theory was Effective Medium Theory (EMT) which tries to explain some of the observed interstellar properties.
Recent space probes have confirmed that the dust grains are bf highly porous and fluffy (i.e. aggregates or clusters) rather than having regular shapes (spherical, cylindrical or spheroidal) and homogeneous in composition and structure. Since their is no exact theory for calculation of scattering properties of such irregular, inhomogeneous particles, our group has used Discrete dipole approximation (DDA) method and the results of this is discussed.

Role of Dust

The model uses a composite fluffy dust grain for explaining most of the observed interstellar extinction curves and also polarization. Another parameter which needs to be constrained by the dust models is the interstellar abundances of Carbon and Silicon which is usually overestimated by the solid dust models but our model predicts closer match to the observed ISM abundances.
Further, our composite dust model also explains the IR emission from circumstellar dust. In the near future, there are a few space missions planned by ISRO and ESA viz. ASTROSAT and GAIA which will provide extensive platform for large coverage of UV sky and render interstellar extinction measurements where above models will be useful.

Dust in Astrophysical & Atmospheric Environments

Dust is a very important constituent in many astrophysical environments – though at most situations, its only 1% of the total mass in the ISM! Despite the fact that dust grains have relatively small contribution to the total mass, the remarkable efficiency with which such grains scatter, absorb, polarize and re-radiate the starlight – ensures that they have significant impact on our views of the universe.

Pillars of Dust

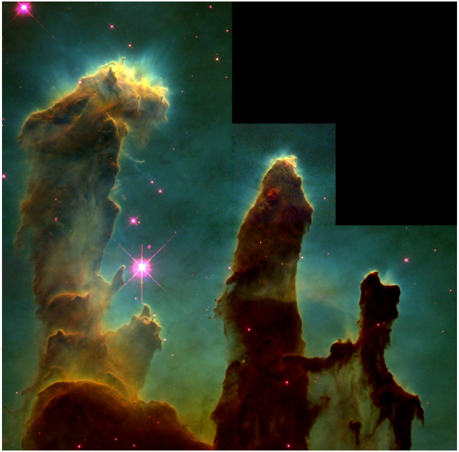

Figure 1: Nebula shows evaporating gaseous globules (EGGs) emerging from pillars of molecular hydrogen gas and dust

Trifid Nebula

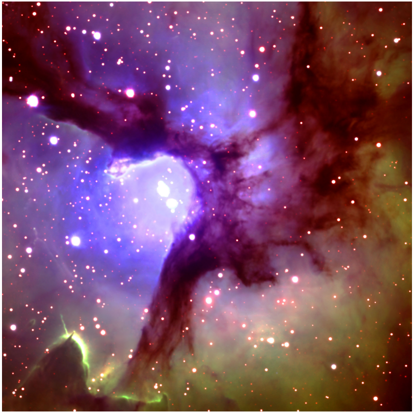

Figure 2: Clouds of glowing gas mingle with lanes of dark dust in the Trifid Nebula, a star forming region towards the constellation of Sagittarius. In the center, the three huge dark dust lanes that give the Trifid its name all come together

Horse Head Nebula

Figure 3: The Horsehead is a plume of dust rising in front of a background of glowing ionized gas off in one part of the Orion Molecular Cloud complex

Sahara Dust Storm

Figure 4: An approaching major dust storm to be followed by a thunder storm and possible rain

Volcanic Dust

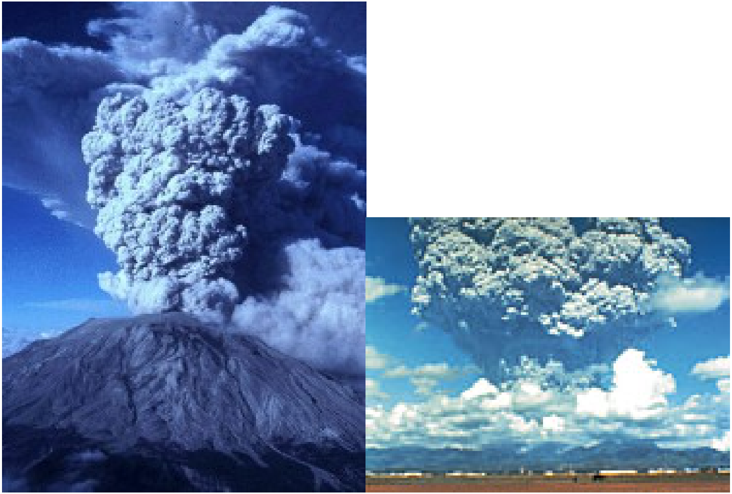

Figure 5: Another source of natural dust – may persist for many weeks – spread all over the globe by winds

Global Warming-Source of man-made dust and its effect on global warming

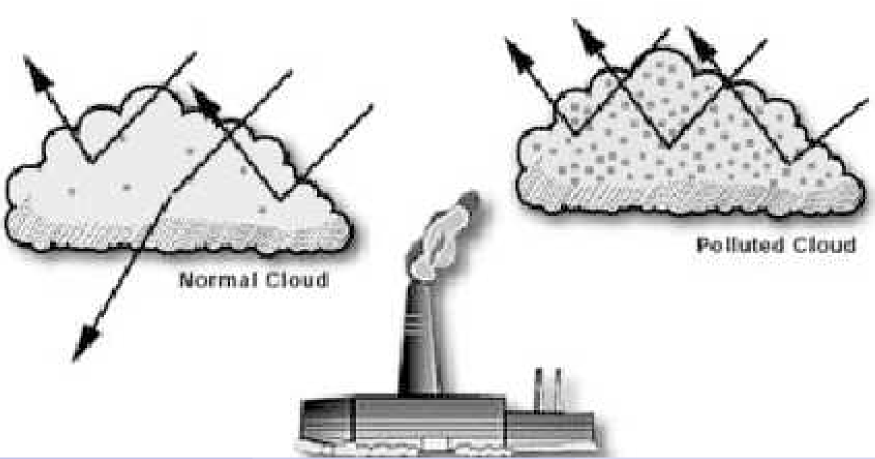

Role of Dust

The main role of dust is to obscure the light from the background source which could be starlight or other general nebulosity. Dust causes the extinction of the background light; affects the polarization and also provides abundance contraints.

All the three aspects:

(1) Extinction

(2) Polarization

(3) Abundance constraints

(4) IR emission in circumstellar dust

have been studied in the past decade by our group.

Further recently, we have used composite silicate grains to explain the IR emission from circumstellar dust.

Light Scattering Basics

- Average total extinction=$\mathrm{A_v} = 1\mathrm{magnitude/kpc}$
- Dust particles radius=$\mathrm{a} \sim \lambda$
- Extinction Law $\propto \lambda^{-1}$
- Extinction Cross-section=$\mathrm{C_{ext}} = \mathrm{Q_{ext}}\pi \mathrm{a}^2$
- Extinction Efficiency=$\mathrm{Q_{ext}} = \mathrm{Q_{sca}} + \mathrm{Q_{abs}}$ (depends on $(2\pi\mathrm{a}/\lambda)$&$(\mathrm{m} = \mathrm{n} - \mathrm{ik})$
- Density of Dust=$\rho \sim 1.2 \times 10^{-23}\mathrm{kgm^{-3}}$
- Gas to Dust Ratio=$\frac{\rho(\mathrm{dustparticles})}{\rho(\mathrm{gas})} \sim 10^{-2}$

Light Scattering Basics...contd

- Number density per unit volume along the line of sight to a distant star $= \mathrm{n_d}$
- Length of Cylinderical Column = L
- Number of Grains contained in a cylinderical column of length L and unit cross-section area $= \mathrm{N_d} = \mathrm{n_d L}$
- If instead of constant radius a, we have a size distribution
  $$\mathrm{N_d} = \int \mathrm{n(a)da}$$

Light Scattering Basics...contd

- Number of Dust grains per unit volume having radius in the range of a and a+da = n(a)da $\propto \mathrm{a}^{-3.5}\mathrm{da}$ (Mathis et.al. 1977 – power law grain size distribution – MRN Law)
- Total Extinction=$\mathrm{A}_\lambda = 1.086\mathrm{N_d C_{ext}} = 1.086\mathrm{N_d}\pi\mathrm{a}^2\mathrm{Q_{ext}}$
  $=1.086\pi \int \mathrm{a}^2\mathrm{Q_{ext}}\mathrm{n(a)da}$
  $=\pi \int_{\mathrm{a1}}^{\mathrm{a2}} \mathrm{a}^2\mathrm{Q_{ext}}\mathrm{a}^{-3.5}\mathrm{da}$

References on Dust Modeling by our group

- Vaidya & Gupta, A & A, <u>328</u>, 634 (1997)
- Vaidya & Gupta, A & A, <u>348</u>, 594 (1999)
- Vaidya, Gupta, Dobbie & Chylek, <u>375</u>, 584 (2001)
- Gupta, Mukai, Vaidya, Sen & Okada, A & A, <u>441</u>, 555 (2005)
- Gupta, Vaidya, Dobbie & Chylek, Astrophys. Sp. Sci., <u>301</u>, 21 (2006)
- Vaidya, Gupta & Snow, MNRAS, <u>371</u>, 791 (2007)
- Vaidya & Gupta, JQSRT, <u>110</u>, 1726 (2009)
- Roy, Sharma & Gupta, JQSRT, <u>110</u>, 1733 (2009)
- Roy, Sharma & Gupta, JQSRT, <u>111</u>, 795 (2010)
- Katyal, Gupta & Vaidya, Earth, Planets and Space (EPS) Journal, <u>63</u>, 1 (2011)
- Vaidya & Gupta, A&A, <u>528</u>, A57 (2011)
- Roy, Sharma, Gupta & Ranadive, JQSRT, <u>113</u>, 624 (2012)

References...contd.

- N. Katyal, R Gupta and D B Vaidya, PASP, 125, No. 934, 1443 (2013)
- P. Shalima, J. Murthy, and R. Gupta, EPS, 65, no. 10, 1123 (2013)
- P. Shalima, Rupjyoti Gogoi, Amit Pathak, Ranjeev Misra, Ranjan Gupta & D. B. Vaidya, PASP, 127, 726 (2015)
- Amritaksha Kar, Asoke K Sen, Ranjan Gupta, ICARUS, 277,300 (2016)
- Ranjan Gupta, Dipak B. Vaidya & Rajeshwari Dutta, MNRAS, 462(1), 867(2016)
- A. K. Sen, R. Botet, R. Vilaplana, Naznin R Choudhury & Ranjan Gupta, JQSRT, 198, 164 (2017)

Spheres v/s Solid Spheroids

- Extinction efficiencies $\mathrm{Q_{ext}(spheroid)/Q_{ext}(sphere)}$
- v/s Wavelength for different grain sizes and axial ratios for Silicate and Graphite grains with T-Matrix.
- **Oblates** have axial ratios > 1.0
- **Prolates** have axial ratios < 1.0
- **Sphere** has axial ratio$=$1.0

Silicate Spheroids

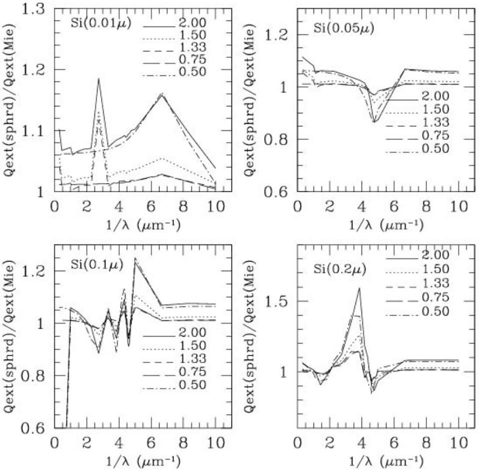

Figure 7: $\mathrm{Q_{ext}}$ ratios for various grain axial ratios and sizes

Graphite Spheroids

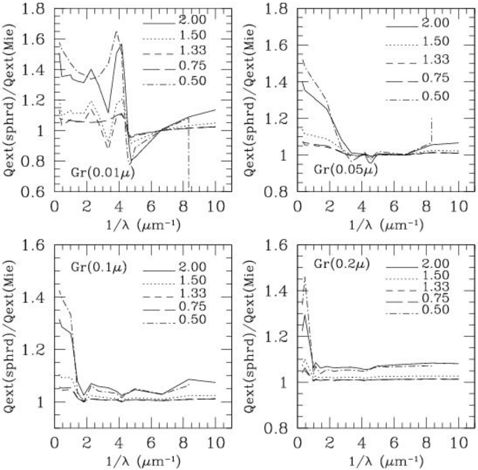

Figure 8: Q_{ext} ratios for various grain axial ratios and sizes

Graphite Bump Region

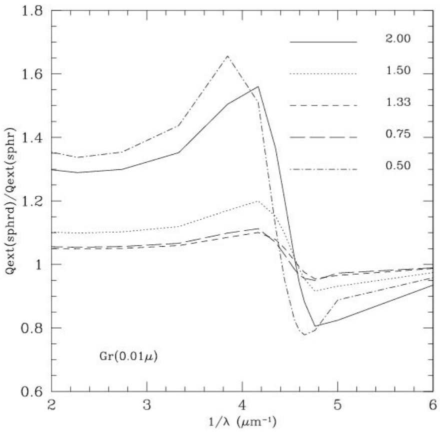

Figure 9: $\mathrm{Q_{ext}}$ ratios for various grain axial ratios and sizes at the UV bump region

Interstellar Extinction Curves (Solid grains)

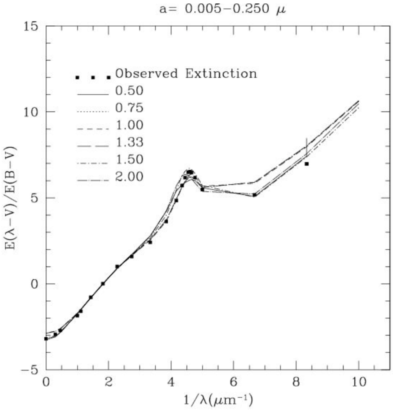

Figure 10: Comparison of Observed Interstellar Extinction curves with the best fit model combination curves of spheroidal silicate and graphite grains with various axial ratios using T-Matrix

Interstellar Extinction Curves (Solid grains)...contd.

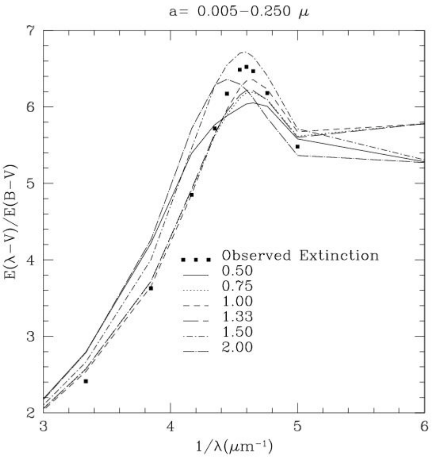

Figure 11: Fitting of Observed Interstellar Extinction Curves at the Bump Region

Extinction and linear polarization (Solid Grains)

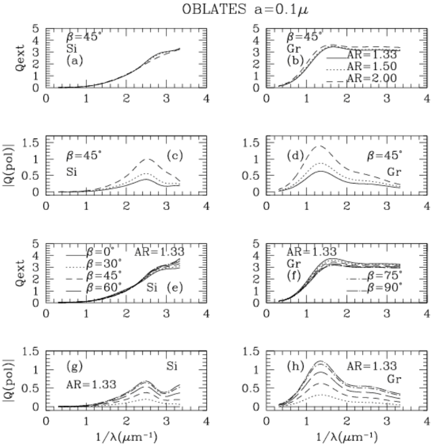

Figure 12: Interstellar Extinction (Q_{ext}) and Linear Polarization (Q_{pol}) for aligned oblate spheroids (silicates and graphites) with grain size a=0.1μ. Various axial ratios (AR) and orientation angles of alignments have been computed

T-Matrix Computations ...contd.

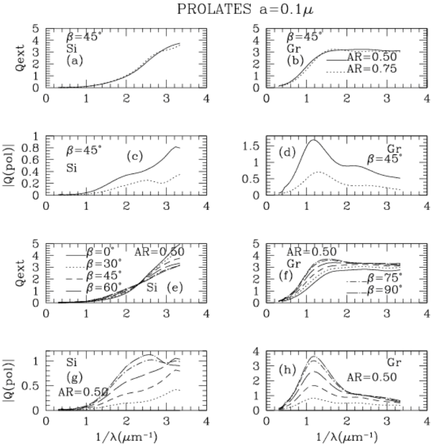

Figure 13: Interstellar Extinction (Q_{ext}) and Linear Polarization (Q_{pol}) for aligned prolate spheroids (silicates and graphites) with grain size a=0.1μ. Various axial ratios (AR) and orientation angles of alignments have been computed

Observed Interstellar Extinction Curve

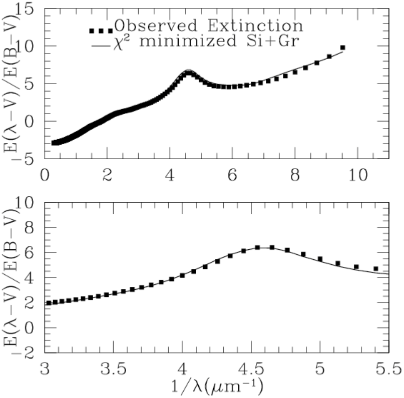

Figure 14: Observed Interstellar Extinction is compared with the best fit model curve of a combination of silicate and graphite grains with axial ratio AR=1.33 using a grain size distribution of 0.005-0.250μ in steps of 0.005μ. Lower panel highlights the UV bump region

EMA & T-Matrix

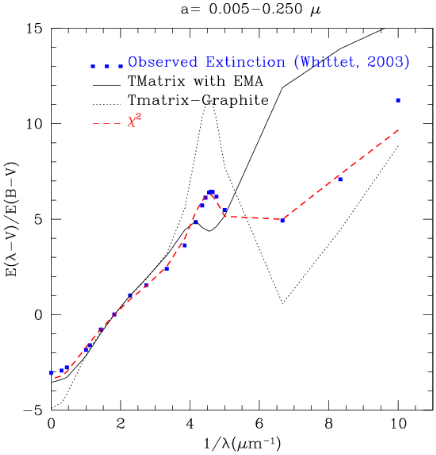

Figure 15: Fitting of Observed Extinction curve with Effective Medium Approximation (Maxwell-Garnet mixing rule) and T-Matrix computation

Discrete-Dipole Approximation (DDA) Basics

Computation for **solid spheres** which are homogeneous and isotropic (cylinders and some more shapes are also possible) could be done by Mie scattering theory. It is clear that dust grains **cannot be solid spheres** or of same composition since observation of interstellar and other polarization requires **non-spherical grains**. T-Matrix and some other exact methods can be used to model non-spherical grains but usually of single composition.

DDA Basics ...contd.

DDA for computing light scattering of particles – originally developed by Purcell & Pennypacker (1973) can handle **non-spherical grains**. DDA replaces the solid grain by an array of N point dipoles, with the spacing between the dipoles small compared to the wavelength. Each dipole has an oscillating polarization in response to BOTH an incident plane wave and the electric fields due to all of the other dipoles in the array (see Draine, ApJ, 333, p848-872, 1988 for more details on DDA method).

"Spherical" Dipole Arrays

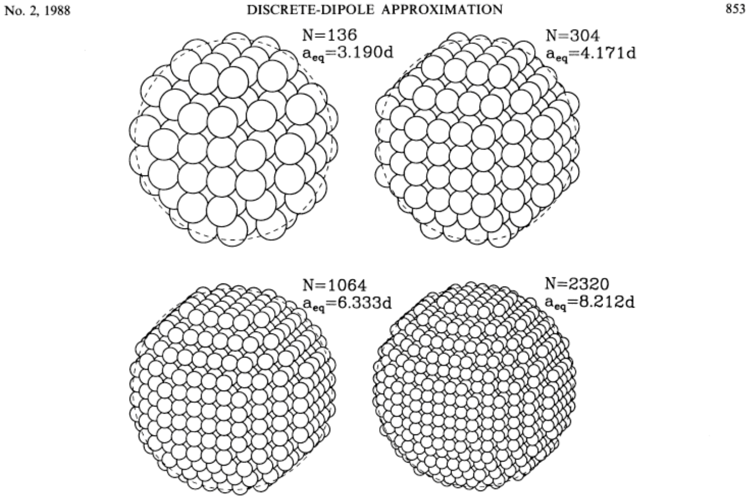

Dipole Polarization within the "Spherical" Arrays

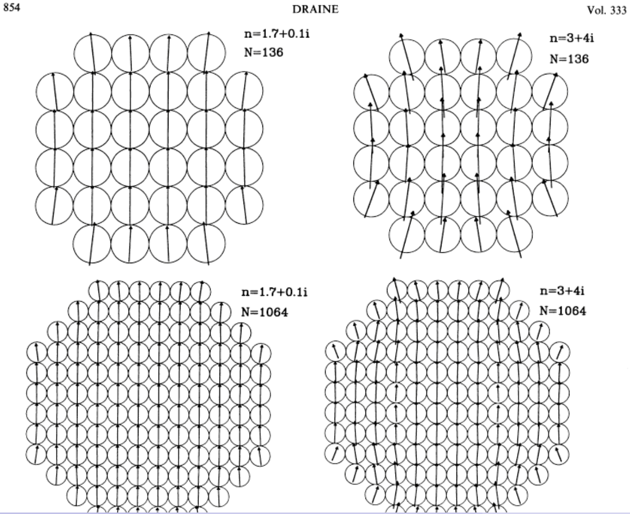

DDA Validity Criteria

Grain volume V is represented by an array of N discrete dipoles – physical size of the grain is characterized by the "equivalent radius" $\mathbf{a_{eq} = (3V/4 * \pi)^{1/3}}$ – i.e. radius of a sphere of equivalent volume. The nearest neighbour distance between the dipoles is $\mathbf{d = a_{eq} * (4 * \pi/3N)^{1/3}}$

(a) The DDA is valid only when the N is large enough (d is small enough compared to the $\mathrm{a_{eq}}$) such that the boundary of the cubic array satisfactorily approximates the desired grain shape.

(b) Another criteria is $\mathbf{|m|kd < 1}$

where m is the complex refractive index; k is π/λ and d is the lattice spacing.

Validity Criteria ...contd.

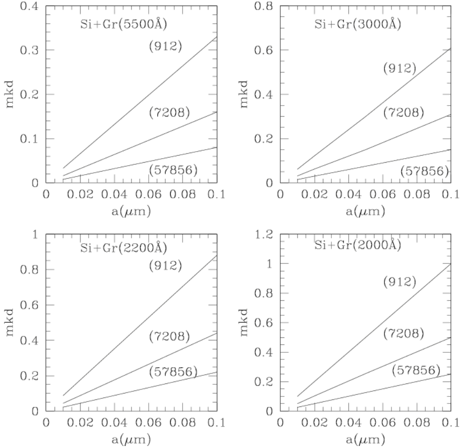

Figure 18: $|\mathrm{m}|\mathrm{kd} < 1$ limits for Si+Gr composite grains with various number of dipoles and wavelength combinations

DDA validity criteria in Optical/UV

λ (μm)	N=9640 a(μ)	14440 a(μ)	25896 a(μ)
3.4000	4.00	5.00	6.00
2.2000	2.50	3.50	4.00
1.0000	1.20	1.40	1.60
0.7000	0.80	1.20	1.00
0.5500	0.60	0.96	0.80
0.3000	0.40	0.50	0.45
0.2000	0.22	0.30	0.25
0.1500	0.14	0.20	0.16
0.1000	0.10	0.16	0.12

Validity Criteria in IR

λ (μm)	N=9640	14440	25896
5.0	0.041	0.030	0.022
10.0	0.021	0.014	0.011
15.0	0.015	0.011	0.005
20.0	0.011	0.007	0.003
25.0	0.005	0.002	0.001

Table 1: Validity criteria in IR region for maximum grain size of a=0.250μ

Porosity

Porosity P is defined as:
$\mathbf{P = 1 - \frac{V_{solid}}{V_{total}}}$ where $\mathrm{V_{solid}}$ is the volume of the solid material inside the grain and $\mathrm{V_{total}}$ is the total volume of the grain.
Porosity varies between $0 < \mathrm{P} < 1$

Axial Ratios & No. of Inclusion (no. of dipoles/inclusion)

Inclusions	Inclusion	Fractions	
N=9640 AR=1.33	f=0.1 32/24/24	f=0.2	f=0.3
16/12/12 *8/6/6* 4/3/3	1(1184) 6(152) 38(16)	2(1184) 11(152) 76(16)	 16(152) 114(16)
N=25896 AR=1.50	f=0.1 48/32/32	f=0.2	f=0.3
12/8/8 6/4/4 3/2/2	7(432) 54(56) 216(8)	13(432) 108(56) 432(8)	19(432) 162(56) 648(8)
N=14440 AR=2.00	f=0.1 48/24/24	f=0.2	f=0.3
16/8/8 *12/6/6* 8/4/4 6/3/3 4/2/2	3(536) 6(224) 23(64) 38(24) 91(8)	6(536) 11(224) 46(64) 76(24) 181(8)	8(536) 16(224) 68(64) 114(24) 271(8)

Table 2: Number of inclusion (and number of dipoles per inclusion)

Orientation Averaging

β from 0 to 180 degrees in 3 steps
θ from 0 to 90 degrees in 3 steps
ϕ from 0 to 180 degress in 3 steps
Total 27 orientations are good enough

Composite Grains

It is very unlikely that interstellar grains have regular shapes (spherical/cylinderical/spheroidal) or that they are homogeneous in compostion and structure. It has been proven that (from balloon observations and other flyby missions) the real dust grains are **porous; fluffy and non-spherical** – rather than solid spheres as was assumed in Mie theory for computation of light scattering properties by dust grains.

Composite Grains

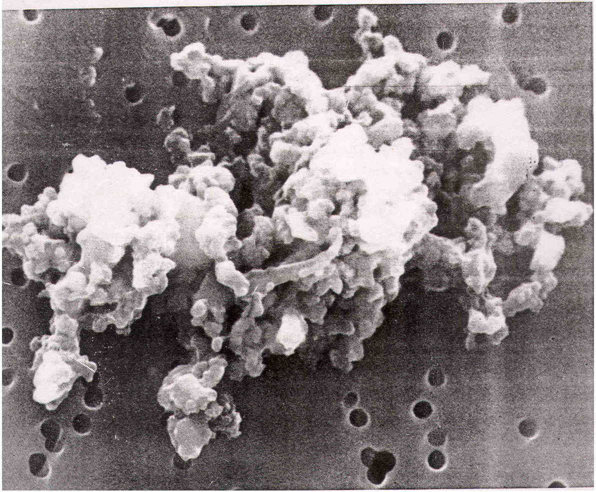

Figure 19: Picture of a Composite Grain

Impact Mission Dust Grains

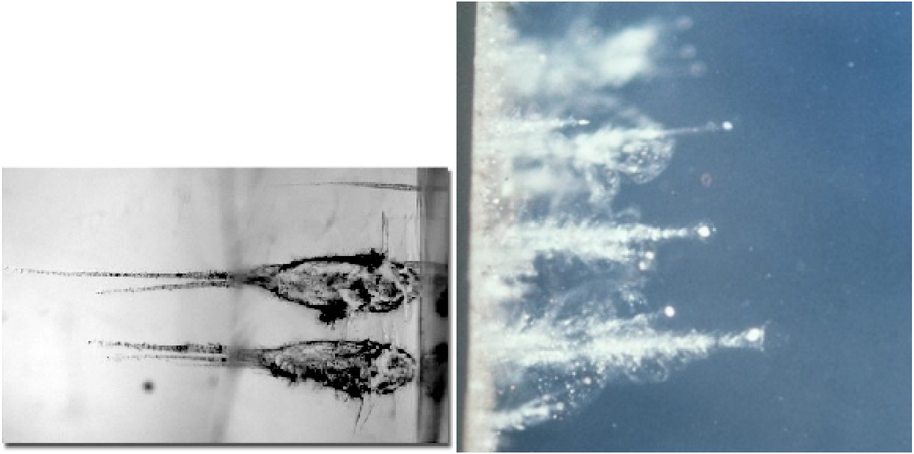

Figure 20: Aerogel Dust Tracks from Impact mission

Multi-component-composite; size distribution and porous etc.

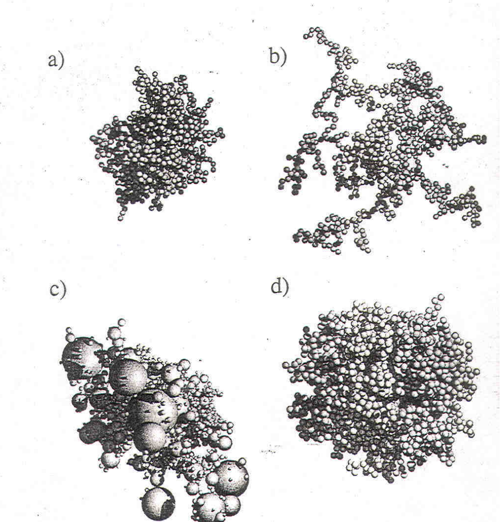

Composite Grains with Inclusions

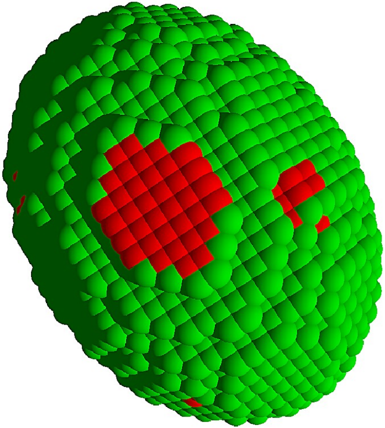

Figure 22: A typical Non-spherical Composite grain with a total of N=9640 dipoles with the inclusions embedded in the host spheroid such that only the ones placed at outer periphery are seen.

Composite Grains with Inclusions ...contd.

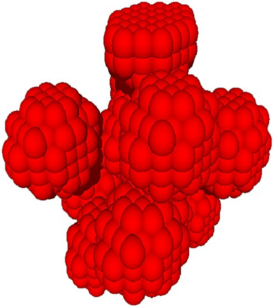

Figure 23: Inclusions

Extinction Efficiencies with Composite Grains

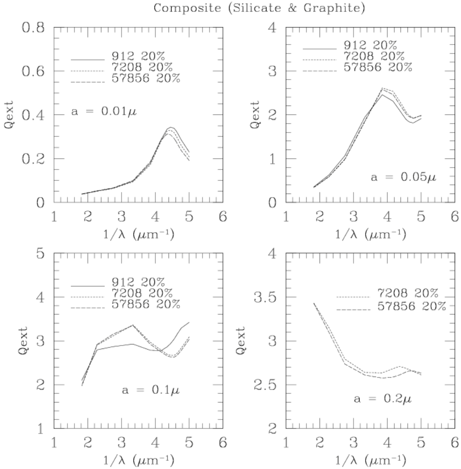

Figure 24: Extinction Efficiencies for Si+Gr Composite Grains with various number of dipoles and grain sizes

Interstellar Extinction ...contd.

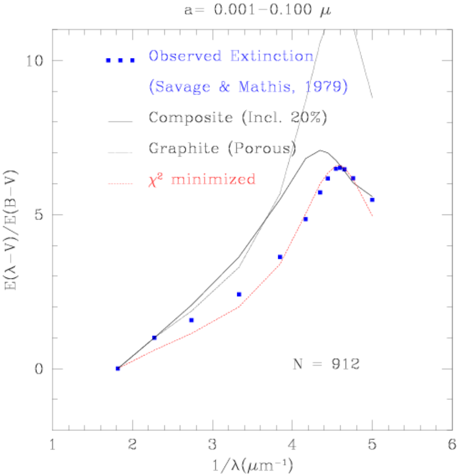

Figure 25: Interstellar Extinction Curve and Model Fitting

Cometary Polarization

3D plots of Scattered Intensity (S11) and Linear Polarization (P) for Composite Spheroidal Grains (N=14440 & 152) with silicate as host sphere and 20% graphite as inclusion. The vertical axes are for S11 and P; the axes marked as θ denotes the Scattering angle (X 10°) in the range 0 to 180° and the third axis is for the grain size a=0.0-1.0μ. The wavelength for these calculations in the K-band at 2.2 μm.

Cometary Polarization ...contd.

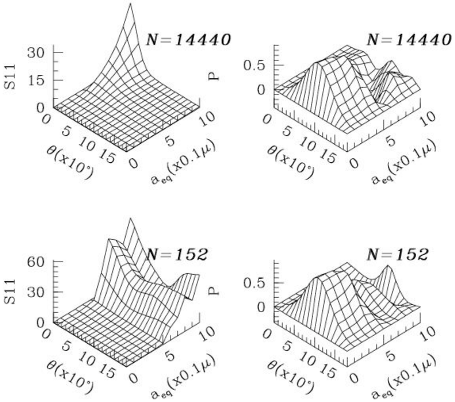

Figure 26: Cometary Polarization

Cometary Polarization ...contd.

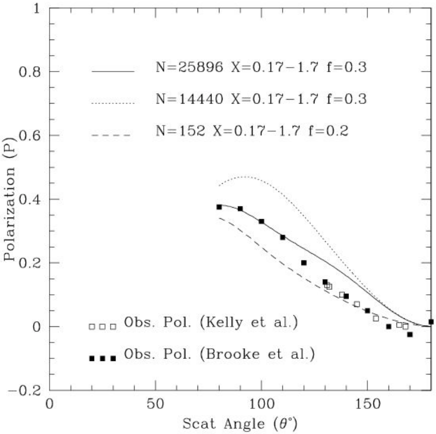

Figure 27: Cometary Polarization

Cometary Polarization

Linear Polarization (P) for Spheroidal Composite Grains (N=25896, 14440 and 152) with silicate as host sphere and graphite as inclusion and comparison with the observed Polarization data for comets.

Note that some comets show the negative branch of polarization at large scattering angles (i.e. $> 150^\circ$) but not all comets show this negative branch in the K-band (Kelly et.al. 2004). Our models do not show this negative branch but the overall curves resemble well with the observations. Calculations are in progress for using fractal aggregate monomers as a model for dust grains which can reproduce the negative branch of polarization.

Fractal Composite Grains

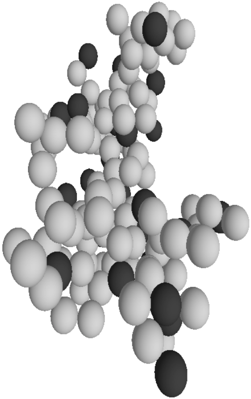

Figure 28: Possible Fractal Grains which can explain negative branch of Cometary Polarization

Interstellar Polarization by Composite Grains

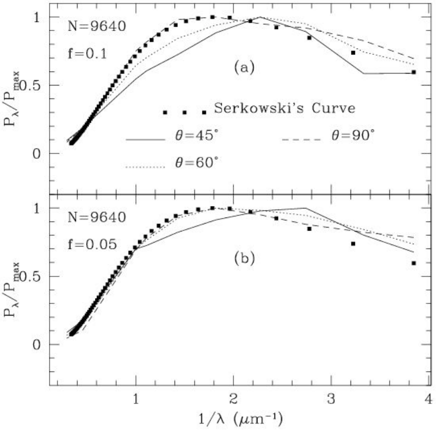

Figure 29: Linear Polarization for N=9640 dipoles and two volume fractions (f=0.05 & 0.10) and comparison with Serkowski's Law

Abundance Constraints & Carbon Crisis

Abundance Ratio (ppm)	ISM	Other Models	Our Model
C/H	110	254	160
Si/H	17	32	25

Table 3: Abundance Ratios

ISM Value: Estimated by Mathis, JGR, 105, 10269 (2000)
Other Models: Li & Draine, ApJ, 554, 778 (2001)
Our Model (Vaidya et al. 2007, MNRAS, 371, 791)

Abundances ...contd.

Calculations with our models predict lower values for Carbon and Silicon abundances as compared to other composite models but a further reduction is warranted to match the estimated ISM values and this could be achieved by introducing a 3rd component in the composite grain like SiC, amorphous carbon and PAH's etc.

The calculations have been done by using the Volume Extinction Coefficient $\mathrm{V_c} = \sum \mathrm{V} / \sum \mathrm{C_{ext}}(\lambda)$ for obtaining the abundances for our models (spheres and spheroids) with various axial ratios and porosities etc.

IR emission from circumstellar dust

Composite grain model has been used to compute IR fluxes in the 5-25μm region at several dust temperatures T=200-350°K and compared with the IRAS-LRS average observed curves and also for two other typical stars which are known to have strong Silicate emission features at 10 and 18 μm.

IR flux comparison with composite models and observed fluxes

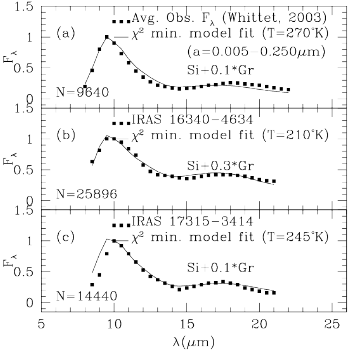

Figure 30: Best fit χ^2 minimized composite grain models (silicates with graphite inclusions) plotted with the average observed infrared flux for IRAS-LRS curve and two other stars

Star Forming Dark Clouds

- Small compact dark clouds (also known as Bok Globules) are undergoing gravitational collapse and may form low mass stars (Bok & Railey 1947).
- These are cold dense clouds of H2, with temperature T$\sim$ 30K, density$=10^4\mathrm{H}_2$ molecules per cm^{-3} and masses 10 to 100 $\mathrm{M}_\odot$, with sizes 1-2 pc
- In order that a cloud contracts towards formation of star(s) the self gravity has to overcome the forces due to thermal outward pressure, rotation in the equatorial plane and magnetic field pressure
- Magnetic field in terms of its strength and geometry plays a key role in collapse dynamics by mediating accretion, collimating the jets and directing out-flows

Dark Clouds ...contd.

- Background star polarimetry provides a good technique to map the magnetic field
- Light from background stars are scattered in forward direction by magnetically aligned dichroic dust grains (Davis & Greenstein 1951)
- The degree and direction of alignment is directly related to the strength and direction of ambient magnetic field in the cloud
- Background star polarimetry provides a technique to probe this magnetic field
- With this aim, we have in the past reported background star polarimetry of such clouds (CB3, 25, 39, 52, 54, 58, 62, 246; Sen et al. 2000)

Dark Clouds ...contd.

- Sen et al. (2005) found that the background star polarization is not independent of the ambient physical conditions within the cloud like temperature, molecular turbulence etc
- Therefore it was concluded that, the polarization measurements can still be used to explore physical conditions within the cloud, though apparently the observed polarization (p) values do not show any relation with extinction values E(B-V)
- To resolve this discrepancy, at this stage one should know the role of grains within the cloud, which are generally held responsible for producing polarization (p) as well as extinction E(B-V). **It seems polarization (p) and extinction E(B-V) are due to two independent grain populations in the dark clouds**
- Observations of these clouds in the UV part of the spectrum may resolve many key issues connected with the role of grains and star formation in general

Polarization & Extinction by Dust

- In order to look for any possible relation between polarization and extinction, we can determine the value of colour excess E(B-V) for each star for which we have the corresponding polarization (p) values available from Sen et al. (2000)
- In order to determine E(B-V) one needs to find the observed magnitudes and spectral types of individual stars
- The background stars are in some cases very faint and the determination of their spectral types is in the process

Dark Cloud CB62 Details - A typical Cloud for this study

- RA(2000) 13:30:02.8
- DEC(2000) $+$79:22:34
- Galactic Latitude *bII* 37.58
- Galactic Longitude *l* 120.69
- Size 3.4 $\times$ 2.2

GALEX Image of CB62

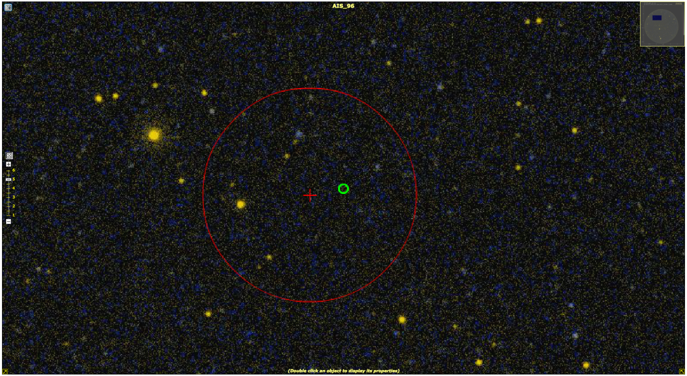

Figure 31: Red Circle shows the UVIT 20arc-min field of view

CB62 Image

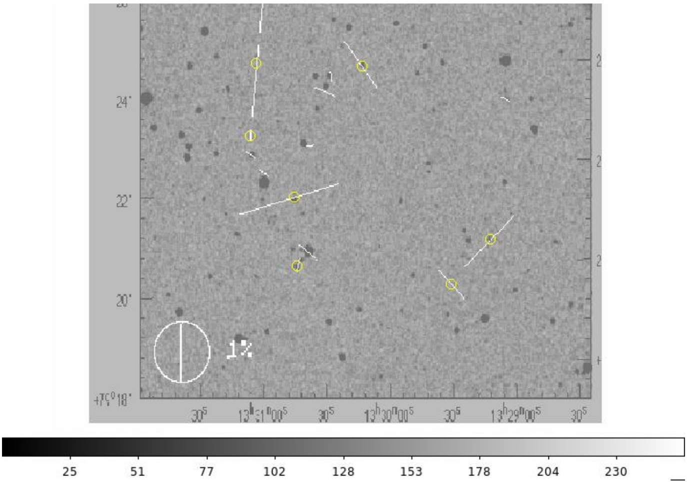

Figure 32: Color Circles show the UVIT target stars & Polarizaton vectors are shown in white bars with their lengths corresponding to the measured linear

CB62 Polarization Measurements

Sr.No.	RA(2000)	DEC(2000)	p(%)	Ep(%)	θ	m
1	13:30:32.2	79:20:23	0.223	0.118	164.7	16.83
2	13:29:23.5	79:19:39	0.664	0.355	43.9	17.34
3	13:30:15.3	79:20:35	0.404	0.249	54.3	14.22
4	13:30:38.9	79:21:49	1.849	0.991	105.1	17.40
5	13:29:10.0	79:20:38	1.186	0.685	132.5	17.37
6	13:30:52.4	79:22:13	0.196	0.126	54.5	13.80
7	13:30:56.8	79:22:41	0.200	0.104	55.4	16.47
8	13:30:29.8	79:22:49	0.125	0.065	99.8	16.60
9	13:30:20.2	79:23:51	0.387	0.203	69.3	17.08
10	13:30:53.9	79:24:46	2.590	1.296	173.4	17.20
11	13:28:51.7	79:23:18	0.149	0.076	62.3	14.01
12	13:30:18.8	79:24:02	0.157	0.101	7.2	16.65
13	13:30:14.0	79:24:16	0.962	0.498	36.9	17.18

Table 4: Observed linear polarization values for various field stars in CB62

Small & Large Dust Grains

- DDA and T-Matrix based light scattering codes used (Gupta et al., 2005)
- Astronomical Silicate dust grains are assumed (Draine et al, 2003)
- Silicate Refractive Index m=1.6904+i0.0288 at $0.55\mu m$ (Visible)
- Silicate Refractive Index m=2.1010+i0.2601 at $0.16\mu m$ (FUV)
- Oblate grains with axial ratio of 1.33
- Grain Orientation 90°

Polarization and Extinction from Dust Model

- Polarization **increases** from 1% to 10% as grain size decreases from 0.55μ to 0.0035μ
- Extinction **decreases** from $\sim$ 2.4 to $\sim$ 0.01 as grain size decreases from 0.55μ to 0.0035μ

$\lambda = 0.55\mu\mathrm{m}$ (Visible)	
Size $\mathrm{a} = 0.55\mu$	$\mathrm{Q_{ext}} = 2.3$
Size $\mathrm{a} = 0.0035\mu$	$\mathrm{Q_{ext}} = 0.003$
$\lambda = 0.16\mu\mathrm{m}$ (FUV)	
Size $\mathrm{a} = 0.55\mu$	$\mathrm{Q_{ext}} = 2.24$
Size $\mathrm{a} = 0.0035\mu$	$\mathrm{Q_{ext}} = 0.04$

Astrophysical Consequence of above

- Thus with the grain sizes **decreasing** – Polarization **increases** but Extinction **decreases** - i.e we propose that there might be two different grain populations are involved
- In Dark Star Forming Clouds:
  Polarization $\Rightarrow$ by Small Grains
  Extinction $\Rightarrow$ by Large Grains
- Based on above findings a case is made here to detect the existence of small grains $(0.0035 - 0.01\mu)$ in the star forming clouds. These particles can be best detected through UV observation as they show far UV excess and characteristic features of 2175Å bump

Need for UV Observations of Dark Clouds

- The UV excess can be detected by the pair method (Fitzpatrick & Massa, 1988)
- $\mathrm{k}(\lambda - \mathrm{V}) = \frac{\mathrm{E}(\lambda - \mathrm{V})}{\mathrm{E}(\mathrm{B}-\mathrm{V})} = \frac{(\mathrm{m}(\lambda-\mathrm{V}) - \mathrm{m}(\lambda-\mathrm{V})_{\mathrm{STD}})}{((\mathrm{B}-\mathrm{V}) - (\mathrm{B}-\mathrm{V})_{\mathrm{STD}})}$
  where $\mathrm{m}(\lambda - \mathrm{V})$ and $(\mathrm{B} - \mathrm{V})$ are the ultraviolet and visual colour of program stars and $\mathrm{m}(\lambda - \mathrm{V})_{\mathrm{STD}}$ and $(\mathrm{B} - \mathrm{V})_{\mathrm{STD}}$ are those of unreddened standard stars
- The standard stars and programme stars should be of the same spectral type
- List of such unreddened standard stars for comparison are available from Fitzpatrick and Massa (1986)
- Photometry and spectrometry of such background stars are required

Polarimetry of Dark Star Forming Cloud CB3

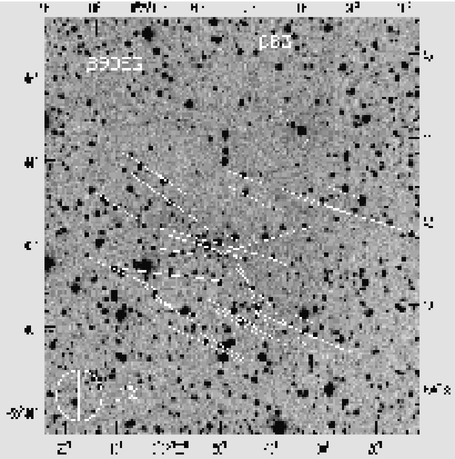

Figure 33: Polarization Vectors tracing the magnetic field along the periphery of dark star forming cloud

Polarimetry of Dark Star Forming Cloud CB25

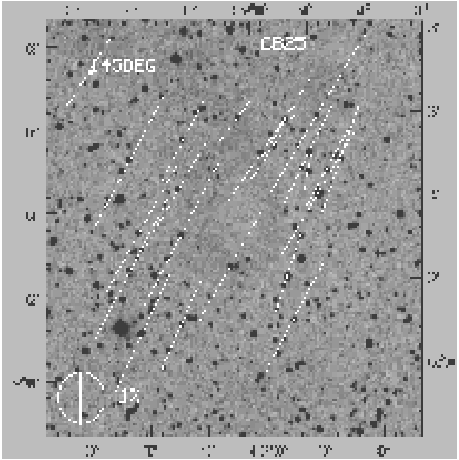

Figure 34: Polarization Vectors tracing the magnetic field along the periphery of dark star forming cloud

Normal BVR Photometry

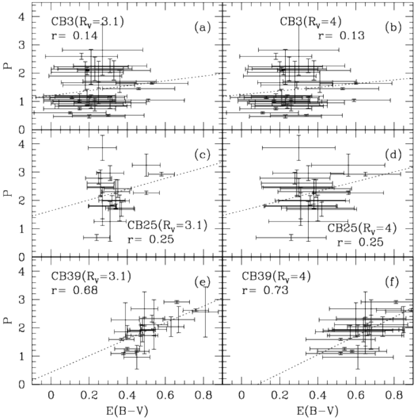

Figure 35: Correlation of Polarization v/s Extinction

Strömgren Photometry

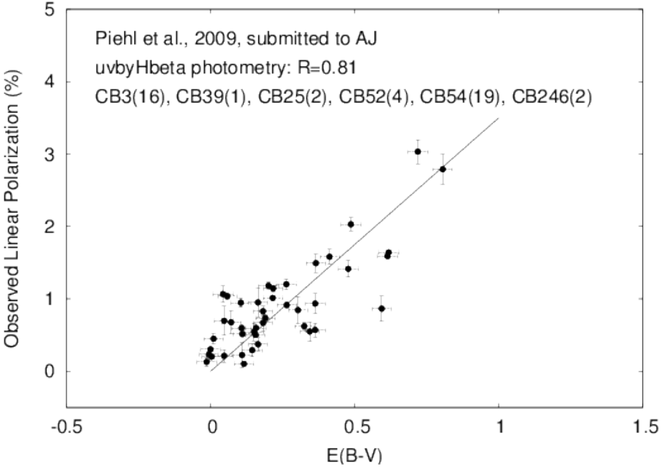

Figure 36: Correlation of Polarization v/s Extinction

Laboratory Studies

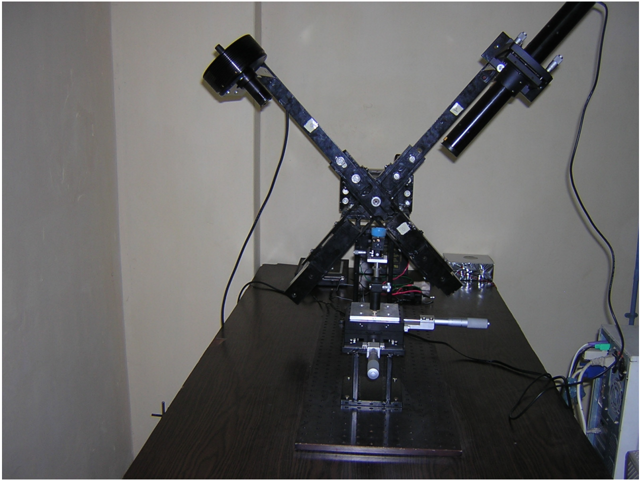

Figure 37: Goniometer fabricated for Assam University, Silchar to study planetary regolith dust analogues

Thanks